

PERSPECTIVE

A recommended “minimum data set” framework for SD-OCT retinal image acquisition and analysis from the Atlas of Retinal Imaging in Alzheimer’s Study (ARIAS)

Jessica Alber^{1,2,3} | Edmund Arthur^{1,2,3} | Stuart Sinoff⁴ | Delia Cabrera DeBuc⁵ | Emily Y. Chew⁶ | Lori Douquette⁷ | Wendy V. Hatch⁸ | Chris Hudson^{8,9} | Amir Kashani¹⁰ | Cecelia S. Lee¹¹ | Stephen Montaquila¹² | Sima Mozdbar¹³ | Leonardo Provetti Cunha^{14,15} | Faryan Tayyari¹⁶ | Gregory Van Stavern¹⁷ | Peter J. Snyder^{1,2}

¹ Department of Biomedical and Pharmaceutical Sciences, University of Rhode Island, Kingston, Rhode Island, USA

² Ryan Institute for Neuroscience, University of Rhode Island, Kingston, Rhode Island, USA

³ Butler Hospital Memory and Aging Program, Providence, Rhode Island, USA

⁴ BayCare Health, Clearwater, Florida, USA

⁵ Bascom Palmer Eye Institute, Department of Ophthalmology, University of Miami, Miami, Florida, USA

⁶ Division of Epidemiology and Clinical Applications, National Eye Institute, National Institutes of Health, Bethesda, Maryland, USA

⁷ Douquette Family Eye Care, Inc., North Smithfield, Rhode Island, USA

⁸ Department of Ophthalmology, University of Toronto, Toronto, Ontario, Canada

⁹ University of Waterloo, Waterloo, Ontario, Canada

¹⁰ USC Roski Eye Institute and USC Ginsburg Institute for Biomedical Therapeutics, Keck School of Medicine of USC, Los Angeles, California, USA

¹¹ Department of Ophthalmology, University of Washington, Seattle, Washington, USA

¹² West Bay Eye Associates, Warwick, Rhode Island, USA

¹³ North Texas Eye Research Institute, Department of Pharmacology & Neuroscience, University of North Texas Health Science Center, Fort Worth, Texas, USA

¹⁴ Department of Ophthalmology, Federal University of Juiz de Fora Medical School, Juiz de Fora, Minas, Gerais, Brazil

¹⁵ Division of Ophthalmology, University of São Paulo Medical School, São Paulo, Minas, Gerais, Brazil

¹⁶ Kensington Eye Institute, Toronto, Ontario, Canada

¹⁷ Department of Ophthalmology and Visual Sciences, Washington University in St. Louis School of Medicine, St. Louis, Missouri, USA

Correspondence

Peter J. Snyder, Office for Vice President of Research and Economic Development, 75 Lower College Road, Kingston, RI, 02881, USA.
E-mail: pjsnyder@uri.edu

Abstract

Introduction: We propose a minimum data set framework for the acquisition and analysis of retinal images for the development of retinal Alzheimer’s disease (AD) biomarkers. Our goal is to describe methodology that will increase concordance across laboratories, so that the broader research community is able to cross-validate findings in parallel, accumulate large databases with normative data across the cognitive aging spectrum, and progress the application of this technology from the discovery stage to the validation stage in the search for sensitive and specific retinal biomarkers in AD.

This is an open access article under the terms of the [Creative Commons Attribution-NonCommercial](https://creativecommons.org/licenses/by-nc/4.0/) License, which permits use, distribution and reproduction in any medium, provided the original work is properly cited and is not used for commercial purposes.

© 2020 The Authors. *Alzheimer’s & Dementia: Diagnosis, Assessment & Disease Monitoring* published by Wiley Periodicals, LLC on behalf of Alzheimer’s Association

Methods: The proposed minimum data set framework is based on the Atlas of Retinal Imaging Study (ARIAS), an ongoing, longitudinal, multi-site observational cohort study. However, the ARIAS protocol has been edited and refined with the expertise of all co-authors, representing 16 institutions, and research groups from three countries, as a first step to address a pressing need identified by experts in neuroscience, neurology, optometry, and ophthalmology at the Retinal Imaging in Alzheimer's Disease (RIAD) conference, convened by the Alzheimer's Association and held in Washington, DC, in May 2019.

Results: Our framework delineates specific imaging protocols and methods of analysis for imaging structural changes in retinal neuronal layers, with optional add-on procedures of fundus autofluorescence to examine beta-amyloid accumulation and optical coherence tomography angiography to examine AD-related changes in the retinal vasculature.

Discussion: This minimum data set represents a first step toward the standardization of retinal imaging data acquisition and analysis in cognitive aging and AD. A standardized approach is essential to move from discovery to validation, and to examine which retinal AD biomarkers may be more sensitive and specific for the different stages of the disease severity spectrum. This approach has worked for other biomarkers in the AD field, such as magnetic resonance imaging; amyloid positron emission tomography; and, more recently, blood proteomics. Potential context of use for retinal AD biomarkers is discussed.

1 | INTRODUCTION

In the current volume of *Alzheimer's & Dementia*, Snyder et al.¹ present the proceedings of an international conference hosted by the Alzheimer's Association in Washington, DC, in May 2019, which brought together experts in Alzheimer's disease (AD) with leading clinicians and researchers in optometry, ophthalmology, and neuro-ophthalmology for a 2-day summit entitled "Retinal Imaging in Alzheimer's Disease." The focus of this meeting was to promote collaborative efforts between AD researchers and retinal specialists in pursuit of the discovery and validation of retinal AD risk biomarkers. Because the retina is an extension of the central nervous system, the development and validation of such biomarkers would allow for a non-invasive, inexpensive, and relatively rapid method for the routine screening of AD risk and progression in large populations of older adults.² Given the lack of preventative or disease-modifying therapies for AD, and the fact that the majority of adults over the age of 40 see an eye care professional intermittently for preventive eye health and vision examinations, correction of refractive error (including presbyopia), and/or ongoing monitoring of ocular abnormalities, retinal screening could serve as a cost-effective, widely accessible method to address a major public health need. This first-ever international conference on retinal imaging in AD identified several key action items or next steps to move retinal AD biomarker research from its current position in the discovery phase to the validation phase. Perhaps the

most critical of these is the need for at least initial agreement on basic standards for data acquisition and analyses, to allow increased opportunities for data sharing across research groups. This will allow researchers in the field to compare imaging data across study cohorts, and eventually would lead to the creation of a widely available comparative reference database, along the lines of the Alzheimer's Disease Neuroimaging Initiative (ADNI³⁻⁵) and the Australian Imaging Biomarkers and Lifestyle Study (AIBL⁶) among other large-scale longitudinal observational trials. These landmark studies have led to massive improvements in how we acquire and interpret neuroimaging and biofluids markers for the disease.

Here, we propose a framework for a "minimum data set" for use in retinal imaging and signal processing across laboratories, based on our collective experience and an exhaustive decision-making process that led to the design of a current multi-site longitudinal observational trial, led by two of us (P.J.S. and S.S.), the Atlas of Retinal Imaging in Alzheimer's Study (ARIAS) that launched recruitment of participants in January 2020. We began with this protocol, and sought input from international experts in this area (all co-authors) to reach a consensus on a recommended minimum data set. Our aim is to propose reproducible methods that can be used across laboratories to aggregate data, cross-validate findings, and accelerate the development of sensitive and specific retinal biomarkers for the early detection of Alzheimer's pathologic change. Although we are well aware that the field is not yet ready to reach a consensus on methods, and that

site-specific differences in the actual optical coherence tomography (OCT) measurements of retinal markers exist due to proprietary differences in manufacturing technologies and processing software. While this cannot be solved with the suggestion of this framework, we are hopeful that publishing this methodology serves as a first step toward finding common approaches that will improve our ability to harmonize data and to cross-validate results across research centers dedicated to the discovery and validation of retinal biomarkers of AD.

1.1 | A proposed framework for a minimum data set in AD biomarker research: spectral domain optical coherence tomography (SD-OCT) image collection and processing

We propose a framework that encompasses structural SD-OCT imaging of the optic disc and the macula, to capture volume and thickness changes of the peripapillary retinal nerve fiber layer (pRNFL), macular retinal nerve fiber layer (mRNFL), ganglion cell layer (GCL), inner plexiform layer (IPL), inner nuclear layer (INL), outer plexiform layer (OPL), outer nuclear layer (ONL), inner and outer photoreceptor segments (IS and OS), and the retinal pigment epithelium (RPE). Because structural changes in the retina in AD have been robustly supported by the growing literature on this topic over the past decade² and all SD-OCT devices support structural retinal imaging, we propose this as a core image acquisition and processing framework. We also propose some additional image acquisition and processing techniques: fundus autofluorescence imaging to examine protein changes and OCT-angiography (OCT-A) of the retinal microvasculature.

As noted above, these methods are being used in the ARIAS trial that is following a large cohort (N = 330) longitudinally for 5 years at three sites in Florida and Rhode Island (NCT# = 03862222). In addition to an extensive retinal imaging protocol, ARIAS will also collect genetic, cognitive, sleep, gait, functional, pupillometry, contrast sensitivity, brain imaging (amyloid positron emission tomography [PET] and magnetic resonance imaging [MRI], for a subset of participants), and blood proteomics data. After completion of data collection and initial analyses, we plan to make this database publicly available as a reference for other researchers, patterned after the data-sharing approach pioneered by ADNI.

1.2 | Instrumental variability across centers and research groups

Multiple instrument manufacturers including, but not limited to, Zeiss, Heidelberg Engineering, Topcon, and Optovue, are all producing very high-quality SD-OCT imaging systems that are in wide clinical and research use worldwide. Although each of these systems produce very similar-looking and high-quality images, technical specifications do vary across these devices that lead to important differences in optics, in-plane resolution, the ability to map point-to-point over successive exams, and many other instrumental differences. Moreover, even

RESEARCH IN CONTEXT

- 1. Systematic review:** The Alzheimer's Association, in partnership with this journal, hosted a first-ever international think-tank meeting on the topic of retinal imaging in Alzheimer's disease (AD) in May 2019, attended by 90 experts from nine countries.¹ One of the key recommendations from the conference was to develop consensus on an initial "minimum data set approach" for future studies, to allow enhanced potential to compare, and/or to coalesce, data collected across multiple laboratories and clinics.
- 2. Interpretation:** This initial attempt at outlining a minimum data set, retinal imaging studies in AD, is based on a large trial that is currently in progress; but that protocol has now been edited and refined with the expertise of all co-authors, representing 16 institutions, and research groups from three countries.
- 3. Future directions:** We hope that this set of recommendations will be considered by, improved, further refined, and adopted by additional research groups and by the new Professional Interest Area (PIA) group of the Alzheimer's Association International Society to Advance Alzheimer's Research and Treatment (ISTAART) that has just recently been launched as another major recommendation from the "Retinal Imaging in AD" conference referenced above.¹

within the same company and SD-OCT system, periodic improvements in their signal processing software packages result in subtle differences in segmentation algorithms, possibly creating an additional source of instrumental variability between labs and between patient visits. It is beyond the scope of this article to recommend how such sources of instrumental error should be addressed when coalescing data across labs, or even within the same center over time. However, we firmly believe that potential between-center main effect differences for vendor/imaging systems need to be thoroughly explored, with multiple research groups working cooperatively, to both collect and then share data sets that can be at least partially merged for statistical analyses, or at least used to derive mathematical equations for conversions between instruments, as has been done previously for diabetic retinopathy.⁷

We are of the opinion that appropriate adjustments will be identified to allow data obtained on one manufacturer's system to be compared reliably to the same type of data obtained on other systems—and this work stream would clearly advance more rapidly with the cooperation of the manufacturers themselves. In the protocol we describe below, we have chosen to use the same Heidelberg Engineering, Inc. (Heidelberg, Germany) SPECTRALIS 2 OCT system at all three clinical sites. Hence, many of the specifications described

below are specific to this particular vendor. We offer this as an example, and would encourage centers relying on imaging systems from other vendors to match the protocol below to accelerate the work of understanding these potential instrument differences.

We also acknowledge that several investigators in academia and industry are developing novel experimental technologies and engineering advances that may supersede some or all of the imaging technologies that we currently rely on, in terms of sensitivity and specificity for AD risk biomarkers (cf. Liu et al.⁸ Yap et al.,⁹ and Braaf et al.¹⁰). Here, we focus on current widely available clinical tools that can be deployed by point-of-care clinicians for validation of retinal biomarkers in the near-term future.

1.3 | Quality control and quality assurance

The veracity of biomarker research, of any type, is utterly dependent on study subject selection and ensuring consistent assurance and quality control (QA/QC), across clinical sites, across technicians and research staff who are collecting data, and across time for within-subjects longitudinal studies. This important set of issues also lies beyond the scope of this article, but the ability to trust any of the retinal imaging biomarkers that we describe below is nonetheless dependent on study designs that effectively ensure proper QA/QC of the data obtained.

1.4 | Structural imaging protocol

The SD-OCT procedures outlined below are currently being performed using the SPECTRALIS HRA + OCT hardware and the Eye Explorer (HEYEX) version 1.10.4.0 (Heidelberg Engineering, Heidelberg, Germany) software with structural, angiographic, autofluorescence, and widefield imaging capabilities. For centers using a Heidelberg SPECTRALIS, the targeted signal quality value of the structural and angiographic images should be at least 20 for the purpose of quality control for image analysis, and an automatic real time (ART) value of at least 7. Prior to imaging, wherever possible, all participants should be dilated with two drops of tropicamide (Mydracil 1%) per eye. There is a 15-minute wait time from drop instillation to image acquisition. We recommend completing all imaging procedures for both the right and the left eye. Doing so allows for the inclusion of research participants who have pathology in a single eye, and provides a margin of error if the image quality is less than optimal for a single eye.

A common approach in retinal imaging research is to rely on a random assignment for each subject enrolled in a given study, to choose either the right eye (*oculus dexter*, OD) or left eye (*oculus sinister*, OS) for data analyses. In practice, the decision to use data from OD versus OS is dependent on the image quality for each eye, participant cooperation during the scanning process, and the presence or absence of ocular pathologies (in each eye) that might adversely impact the quality of the SD-OCT measurements. In Table 1, we provide a listing of ocular and retinal pathologies that, if of sufficient severity so as to limit the quality of imaging data, would result in choosing one eye over the

other (or, in the presence of substantial bilateral ocular disease, would exclude a participant from the study altogether). In at least some cases, ophthalmic evaluation is necessary to evaluate the disease severity and to develop reproducible inclusion and exclusion criteria.

For structural OCT imaging, to avoid inter- and intra-subject thickness measurement biases due to axial length,¹¹ we correct using a modified Littman's formula, which is currently in use by several investigators in this field.¹² For sites unable to measure axial length, participants with <or >5.0 diopters native spherical equivalent should be excluded. Additionally, although regulations surrounding storage of demographic information vary regionally, nationally, and internationally, we recommend collecting the following demographic variables as a minimum: age, years of education, race, sex. All of these factors can affect retinal morphology and/or cognition in AD, and may be required as covariates in analyses examining between- or within-subject comparisons.

1.4.1 | Structural SD-OCT imaging at optic disc

For research groups relying on the imaging system produced by Heidelberg Engineering, the SPECTRALIS HRA + OCT glaucoma imaging module should be used, centered on the optic disc, consisting of three concentric circles of diameters 3.5, 4.1, and 4.7 mm. This imaging protocol should be completed in high-speed (HS) mode, with 27 B-scans for each of the three concentric circles and 30 frames averaged per each B-scan location. Segmentation is completed automatically with HEYEX software. For centers relying on systems produced by other companies, we recommend working closely with each vendor to match these measurement diameters around the optic disc. Additionally, the automatic segmentation results may be validated by periodic batches of manual segmentation.

1.4.2 | Outcome variables and analysis

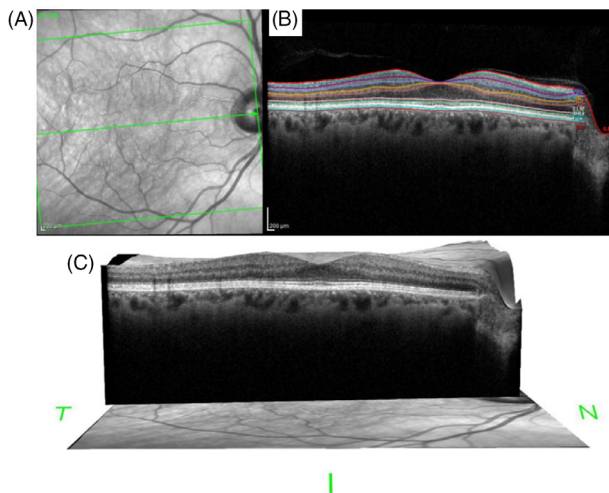
pRNFL thickness is the variable of interest with respect to optic disc imaging, due to the evidence in the literature indicating changes to the pRNFL in AD.^{13,14} Outcome variables include the average pRNFL thickness (in microns) in the seven standard glaucoma fields centered on the optic disc (global average [G], temporal [T, 315-45°], temporal superior [TS, 45-90°], temporal inferior [TI, 90-135°], nasal [N, 135-225°], nasal superior [NS, 225-270°], and nasal inferior [270-315°]) in each of the three concentric circles. In addition, a progression model to assess the longitudinal change in the global pRNFL thickness in each of the three concentric circles (3.5, 4.1, and 4.7 mm) is completed for each participant. Notably, these fields may differ slightly among commercial vendors.

1.4.3 | Structural SD-OCT imaging at the macula

Our standard protocol uses the preset posterior-pole imaging module on the SPECTRALIS, with fixation on the fovea. This protocol

TABLE 1 List of ocular pathologies that influences choice of either eye or exclusion of participants altogether in the event of a bilateral condition for the purpose of image analysis

Anterior segment conditions	Posterior segment conditions
Dense cataracts (that impede image quality)	Age-related macular degeneration
Corneal disease affecting media visualization or opacity	Diabetic retinopathy
Unusually high myopia/refractive errors (>or <5.0 diopters) native spherical equivalent, substantial media opacity, or corneal disease that may provide accurate visualization of the retinal fundus	Hypertensive retinopathy
Anterior uveitis	Other retinal vascular diseases, eg, retinal ischemic changes, central (or branch) retinal vein occlusion, central (or branch) retinal artery occlusion, retinal vasculitis
	Macular diseases, eg, epiretinal membrane, macular hole, vitreomacular traction syndrome
	High myopic eyes associated with posterior staphyloma
	Glaucoma
	Optic nerve disease, eg, optic disc edema, inflammatory, ischemic, compressive, hereditary, toxic, and nutritional optic neuropathies
	Cystoid macular edema
	Substantial media opacity, eg, floaters, asteroid hyalosis, vitreous hemorrhage
	History of retinal or macular surgery in the past 6 months
	Posterior uveitis
	History of intravitreal injections

**FIGURE 1** A composite diagram showing a 30 × 25 degree spectral domain optical coherence tomography (SD-OCT) grid centered on the macula with an individual SD-OCT scan through the fovea (61 B-scans, 123 microns between B-scans; A, a segmented foveal B-scan, with retinal neuronal layers delineated [B], and a 3D representation of the foveal B-scan in space [C]). T, N, I, represent the temporal, nasal, and inferior portions of the retina respectively. Figure by Dr. E Arthur

encompasses a macular centered SD-OCT grid of size 30° × 25° (~8.8 × 7.4 mm) with 61 B-scans across the macula, 123 microns spacing between B-scans, and 10 frames averaged per each B-scan location (see Figure 1). The HEYEX software automatically segments and

computes the thickness of all retinal layers. Recent work shows that this automated software segmentation has excellent agreement with trained observers in evaluating retinal layer boundaries and thicknesses in patients with neurodegenerative disease.¹⁵ For quality control purposes, obvious errors in segmentation lines are manually corrected in all B scans spanning a 6 mm Early Treatment Diabetic Retinopathy Study (EDTRS) grid. Examples of obvious errors, following Wong et al.,¹⁵ include errors visible on quick inspection due to image acquisition errors or pathology. Again, similarly high-quality macular structural imaging may be obtained from all differing types of current SD-OCT systems that are in use by research centers around the world.

1.4.4 | Outcome variables and analysis

Most software to support the OCT systems offered by any major vendor, including Heidelberg's HEYEX software, will automatically compute retinal layer thicknesses (in microns) of the mRNFL, GCL, IPL, INL, OPL, ONL, IS and OS, and the RPE. The retinal layer segmentation algorithm of the HEYEX software has been validated against manual segmentation previously in neurodegenerative disease.¹⁵ Volume measurements (in mm³) of all the above-mentioned retinal layers may also be computed. An ETDRS map consisting of three concentric circles of diameters 1, 3, and 6 mm centered on the macula is produced automatically by the HEYEX software (ETDRS, 1991). The ETDRS map is a pseudo-color thickness map providing average retinal thickness and volume measurements of the above-mentioned retinal layers for the fovea, inner, and outer retinal regions corresponding to the

1, 3, and 6 mm diameter circles, respectively, centered on the fovea. Inner and outer retinal layer thicknesses are considered because these layers have been indicated to remodel with AD.^{16–20} The inner and outer regions are both divided into the superior, inferior, nasal, and temporal portions, which, when combined with the foveal region adds up to a retinal thickness map of nine regions (ETDRS, 1991). The accurate centering of the ETDRS map on the fovea of all study participants is verified by the retinal photographer to ensure accurate retinal thickness values of the retinal layers for all nine regions.

In addition to analysis of the ETDRS grid, we analyze an 8 × 8 mm posterior pole grid centered on the macula. We use Heidelberg's HEYEX software with NSite Analytics[®] to compute the retinal thickness values of all of the retinal layers for the 64 boxes within the 8 × 8 mm posterior pole grid. This provides a more localized analysis of retinal layer thickness across the macula, rather than relying on average volume and thickness. Software analytics packages designed to work with imaging systems from other manufacturers will provide very similar metrics.

1.5 | Additional imaging modalities

While research on structural retinal biomarkers in AD is furthest along in terms of discovery work, there is an expanding body of literature elucidating changes in retinal proteinopathies and the retinal vasculature in AD, with the hopes of creating sensitive and specific biomarkers to detect AD risk and monitor disease progression. At this point, it is unknown which retinal biomarker, or combination thereof, will be useful at each stage of the neurodegenerative continuum. Here, we list imaging acquisition and analysis procedures for the ARIAS trial to examine retinal A β and retinal vascular changes in cognitively normal older adults, mild cognitive impairment (MCI) patients, and mild AD patients.

1.6 | Retinal amyloid beta (A β): autofluorescence imaging

Autofluorescence imaging is available within the Heidelberg SPECTRALIS system to examine the presence of A β in the retinal neuronal layers. We use a 55° widefield lens to acquire fundus autofluorescence (FAF) images of the central, superior, and inferior retina of all study participants using SPECTRALIS confocal scanning laser ophthalmoscopy (cSLO). The wider lens is used to capture a larger surface area and to search for putative evidence of amyloidosis in the periphery. If this lens is not available, use of the standard lens is appropriate for this data, as long as the lens and field of view are specified at the time of dissemination of results. The composite image is then evaluated for number and surface area of inclusion bodies suspected to contain amyloid proteins.^{21,22} Retinal inclusion bodies have been previously found in the retina of preclinical AD research participants, with the number and surface area of these inclusion bodies being moderately correlated with a standard index of amyloid aggregation on PET brain

imaging.²³ In symptomatic AD patients, fundus autofluorescence with SLO has been used to quantify retinal amyloid *in vivo*, and confirmed by autopsy.^{24–26}

1.7 | Outcome variables and analysis

We use the Heidelberg Explorer (HE) region finder tool of the HEYEX software to compute the number count and total surface area of the inclusion bodies in the autofluorescence images. This tool allows the operator to place a seed in an area of interest, and the software automatically computes the boundary of the object. On visual inspection, the rater has the ability to modify the boundaries as required. All images are read by two qualified and independent raters, and we exclude the 360-degree region within 1 disc diameter from the center of the optic disc and the 360-degree macular region within 1 disc diameter of the foveal center. This is done to avoid including the area of hypopigmentation around the optic nerve in participants with zone α or β crescents or peripapillary atrophy and to avoid inclusion of age-related macular drusen in these two regions. Inclusion bodies are only counted if they reach 100% consensus ratings in two independent raters, who are blind to participant information, including demographics, medical history, and clinical status.

2 | RETINAL ANGIOGRAPHIC CHANGES: OPTICAL COHERENCE TOMOGRAPHY ANGIOGRAPHY (OCT-A) IMAGING

We collect a macular centered 20° × 20° (6 × 6 mm) OCTA image consisting of 512 B-scans, with 12 micron spacing between B-scans, and five frames averaged per each B-scan location for each participant. This produces the superficial vascular complex (SVC) angiogram, defined as the composite retinal vascular plexus from the inner limiting membrane to the IPL using HEYEX software. Although not exactly the same, similar scan parameters are available on other commercial platforms as shown in Table 2.

2.1 | Outcome variables and analysis

The outcome variables measured from the OCT-A images include foveal avascular zone (FAZ) size, capillary density, capillary non-perfusion area, and multifractal properties as measured by the generalized dimension and singularity spectra. All of these metrics appear to be influenced by the presence of AD.^{27–29}

At the present time, there is little broad agreement on how best to process the highly complex OCT-A imaging data that can now be easily acquired, as processing technology is still relatively new. There is a rapidly growing number of published methods for OCT-A signal analyses and data reporting, and currently little agreement on standard metrics. MarkVCID represents an ongoing multicenter initiative to develop consensus methodology for OCTA in the assessment of

TABLE 2 Summary of the retinal imaging modalities, techniques of retinal image analysis, and outcome variables, using Heidelberg SPECTRALIS and Zeiss equipment. Specifications provided for each manufacturer are exemplars; there are additional manufacturers of quality SD-OCT equipment that are not listed. For individual system specifications, for each manufacturer, see Schott⁴²

Retinal imaging modality	Number of B-scans	Size of field	Image analysis technique	Processing software	Outcome variables	Reported findings in AD ^b
Proposed "Minimum Data Set" Structural SD-OCT imaging at optic disc (2 to 5 minutes for OS and OD)	27	3.5, 4.1, and, 4.7 mm diameter concentric circles centered on the optic disc	HRA + OCT	Heidelberg Eye Explorer with N-Site Analytics	pRNFL thickness in the seven glaucoma standard fields	pRNFL thinning
	200	3.4 mm diameter concentric circle centered on the optic disc 6 × 6 mm	Optic Disc Cube 200 × 200	Zeiss Cirrus Optic Nerve Analysis Software	pRNFL thickness, disc area, cup-to-disc ratio	
	256 (128)	3.4 mm diameter annulus centered on the optic disc 6 × 6 mm	TABS Segmentation ⁴³	Topcon Fastmap and IMAGENet 6 Software	pRNFL thickness in the clockhour, quadrant, and overall average glaucoma standard fields, disc area, cup-to-disc ratio	
Structural SD-OCT imaging at the macula (2 to 5 minutes for OS and OD)	61	30° × 25° (~8.8 × 7.4 mm) SD-OCT grid centered on the macular	HRA+OCT	Heidelberg Eye Explorer, glaucoma module	All individual retinal layer ^c thicknesses and volume in the nine field ETDRS map	mRNFL thinning, GC-IPL thinning, structural changes associated with cerebral biomarker and cognitive changes
	128	6 × 6 mm SD-OCT grid centered on the macula	Macular Cube Scan 512 × 128	Zeiss Cirrus Macular Analysis Software	All individual retinal layer ^c thicknesses and volumes in the nine field ETDRS map	
	256 (128)	6 × 6 mm or 7 × 7 mm SD-OCT grid centered on the macula	TABS Segmentation ⁴³	Topcon Fastmap and IMAGENet 6 Software	Full retinal thickness in the nine field ETDRS map, and ganglion cell thicknesses in the macula six grid	
Widefield autofluorescence imaging (8 to 10 minutes for OS and OD)	NA	55° ^a	cSLO, blue light autofluorescence	Heidelberg Eye Explorer, HE Region Finder	Surface area and volume of inclusion bodies	Aβ aggregation, tau aggregation, associated with cerebral Aβ, tau
Optical Coherence Tomography Angiography imaging at the macula (8 to 10 minutes for OS and OD)	512	20° × 20° (6 × 6 mm) SD-OCT grid centered on the macular	OCT-A	Heidelberg Eye Explorer, custom programming software (MatLab, Mathworks), Image processing software (Image J)	FAZ size, capillary density, capillary nonperfusion, multifractal dimension	Enlarged FAZ, reduced vessel branching, tortuosity, density, reduced blood flow
	128	3 × 3 mm or 6 × 6 mm SD-OCT grid centered on the macula	OCT-A	Zeiss Cirrus Angioplex Software, custom software (Matlab, Mathworks), and ImageJ	FAZ size, capillary density, capillary nonperfusion, fractal dimension	

(Continues)

TABLE 2 (Continued)

Retinal imaging modality	Number of B-scans	Size of field	Image analysis technique	Processing software	Outcome variables	Reported findings in AD ^b
	320 or 512	3 × 3 mm, 4.5 × 4.5 mm, 6 × 6 mm, 9 × 9 mm, 12 × 12 mm SS-OCT scan area centered on the macula or disc	OCT-A	Topcon Fastmap and IMAGENet 6 Software	FAZ measures (area, perimeter, circularity), macular and RPC vessel densities	

Abbreviations: A β , amyloid beta; AD, Alzheimer's disease; cSLO, confocal scanning laser ophthalmoscopy; ETDRS: Early Treatment Diabetic Retinopathy Study; FAZ, foveal avascular zone; NA, not applicable; OD, oculus dexter; OS, oculus sinister; pRNFL, peripapillary retinal nerve fiber layer; RPC, radial peripapillary capillary; SD-OCT, spectral domain optical coherence tomography; SS-OCT, swept source optical coherence tomograph.

^aWidefield (55 deg) lens should be used if available.

^bSee Alber et al.² for review.

^cRetinal layers include macular retinal nerve fiber layer (mRNFL), ganglion cell layer (GCL), inner plexiform layer (IPL), inner nuclear layer (INL), outer plexiform layer (OPL), outer nuclear layer (ONL), inner and outer photoreceptor segments (IS and OS), and the retinal pigment epithelium (RPE).

vascular cognitive impairment or dementia. The methodology of this study will soon be available and will likely aid in the harmonization of angiography data. Below, we offer one approach that our group is focusing on, as these methods may be reproduced with relative ease using widely available software, as described below.

The HEYEX software lasso tool is used to delineate the borders of the FAZ, to allow for surface area measurement on the SVC image. After this, we export the SVC images as tiff files into custom programming software (Matlab, Mathworks) for further image processing and analysis. First, a vesselness filter is applied to the images^{30,31} to increase the probability of resolving a vessel at a specific location in the image when it is actually present versus noise or motion artifact. Next, the Otsu thresholding method³² is applied to the resultant image to reduce background noise. After the thresholding, we use a customized program script³³ to count the number of pixels designated as vessels. These thresholding and pixel counting methods are applicable to all OCTA images, regardless of device used for acquisition. The number of pixels is then converted into mm² based on the micron-to-pixel ratio in the x and y directions, as computed from the fiducial marks acquired from the HEYEX software. The resultant value in mm² is the capillary density in the SVC. To compute the area of non-perfusion, we subtract the computed capillary density from the known area of the SVC angiogram (36 mm²).

To investigate the fractal properties of the retinal vascular network in the processed SVC angiogram, all images are analyzed using the image processing software Image J (Wayne Rasband, National Institutes of Health in Bethesda, Maryland, USA) together with the FracLac plugin (A. Karperien—Charles Sturt University, Australia). We compute the multifractal properties of the retinal vascular plexus in the SVC using the generalized dimension and singularity spectra.^{28,29,34,35} Several other analysis platforms are available either from other commercial vendors or research groups specializing in angiography analysis.³⁶

Table 2 summarizes the retinal imaging modalities of this framework, techniques for retinal image analysis, and outcome variables for our suggested methodological framework.

3 | SUMMARY AND DISCUSSION

Here, we suggest a reproducible methodology to serve as a recommended “minimum data set” for collection and analysis of retinal images in AD research, in hopes of harmonizing data to generate rapid discovery and moving the field toward validating sensitive and specific retinal biomarkers for AD risk and to monitor disease progression. This recommended protocol is offered as a starting point to address one of the key needs identified by experts from academia, industry, federal agencies, and regulatory authorities at the May 2019 Retinal Imaging in Alzheimer's Disease Summit, organized by the Alzheimer's Association.

Our primary focus for the recommended minimum data set is structural retinal changes, measured via retinal neuronal layer thickness and volume and assessed with SD-OCT. This has been extensively reviewed in the literature,^{2,37} using common imaging procedures and techniques in clinical optometry and ophthalmology practice.

We added additional methodology and outcome measures for the assessment of retinal amyloid, and retinal angiography. Although these latter imaging approaches currently require more specialized equipment that is less widely available, several laboratories are currently exploring both protein-related and angiographic retinal changes across the AD spectrum. The techniques used by laboratories in these areas vary, sometimes considerably, across laboratory groups. Our hope is this recommended minimum data set represent a first step toward galvanizing researchers to align protocols for retinal imaging biomarker research in AD.

To generate this recommended minimum data set, we began with a protocol developed in consultation with industrial and academic experts for and currently used in the ARIAS study (PIs: Snyder, Sinoff). We consulted with national and international experts to expand upon and modify this protocol, resulting in the above recommended minimum data set for retinal imaging biomarker discovery research in AD. Our goal is to increase methodological concordance across laboratories, so that the broader research community is able to cross-validate findings in parallel, accumulate large databases with normative data across the cognitive aging spectrum, and progress from the discovery stage to the validation stage in terms of retinal biomarker development for AD.

Although we believe this framework makes a start at filling an unmet need in the field, we understand that this is a first step in working toward reliable methodological harmonization across laboratories, and that many additional steps must be taken to achieve true methodological concordance across labs in academia, the clinic, and in industry. We acknowledge that this minimum data set will not necessarily be applicable across all devices and manufacturers, and that solving technological and technical variations, even subtle ones due to software variations in the same device, will require co-operation and data-sharing across federal and regulatory agencies, experts in academia and industry, and device manufacturers. Some of the software described in this minimum data set is not part of the “standard” Heidelberg software package (NSite Analytics, OCT-A, Widefield Imaging Module, HE Region Finder tool, see Table 2), and acquisition of this software incurs additional costs, which may not be feasible for all research laboratories. One potential strategy to expedite data sharing is providing access to real raw image data, without any post-processing. Although this would require cooperation of device manufacturers, working with these data would be helpful in terms of expediting collaborative efforts and cross-validation in the field. To that end, there are free image reading platforms available that often produce comparable results to the vendor software, including Ometto et al.’s ReLayer³⁸ software and the National Institutes of Health’s Image J software. SD-OCT images on the SPECTRALIS can be exported as .tiff files instead of HEYEX software’s standard .E2E files. The .tiff file formats can be viewed by any non-proprietary image software, such as Image J, to decouple reliance on proprietary software and pre-/post-processing. These platforms will help to advance the field toward sharing raw, unprocessed SD-OCT data and retinal images, especially in cases in which vendor specific software is not available or not affordable.

The field will need to address additional methodological barriers to produce validated, clinically meaningful and applicable biomarkers. Both AD and cancer have seen success in public–private partnerships, which can be leveraged for the advancement of retinal biomarker validation in AD. As one example, O’Bryant et al.⁴¹ proposed a pathway for the advancement of plasma biomarkers from discovery to clinic, including public–private partnerships, which could be applied to retinal biomarkers in the future. Finally, we expect future retinal biomarker discovery work in academia to modify our recommendations for a minimum data set framework as the pace and popularity of this work in AD increases. This framework is not meant to be exhaustive, but rather a starting point from which to move forward as a field. For example, methodological factors, such as lighting,^{39,40} may influence retinal morphology. As such, standardization of lighting conditions may require standardization in the future, although whether this makes a significant difference in AD measurements remains to be systematically investigated.

Looking to the future, use of this minimum data set could spur efficient data accumulation and analysis in the field, including data examining within subjects, longitudinal change in cognitive aging, and AD. These data are essential to move from discovery to validation, and to examine which retinal AD biomarkers may be sensitive and specific for the different stages of the cognitive aging continuum. This approach has been successful in validating other biomarkers for AD, such as MRI, amyloid PET, and blood proteomics. Moreover, designating an appropriate context of use for structural, protein-related, and microvascular retinal biomarkers will be essential to move the field forward. There are many potential contexts of use for these biomarkers, including, but not limited to, point-of-care screening, risk for pre-clinical AD or risk of progression from MCI to AD, monitoring, diagnosis, or prognosis. Clinical applicability of these biomarkers will depend on context of use; for example, structural retinal biomarkers have been studied extensively in AD patients versus age-matched cognitively normal older adults; however, investigations of these biomarkers in the preclinical AD population remains limited. It is essential to determine at which stage of the cognitive aging continuum these retinal biomarkers are most reliable and accurate, and how they would most efficiently be deployed in clinical practice. In the future, retinal imaging could be deployed as a tool for large-scale screening of cognitively normal older adults. As a field, our goals should center on precision medicine approaches for AD diagnosis and monitoring by minimizing clinician burden; maximizing clinical utility; and identifying individuals at risk for AD for further specialist evaluation and more invasive, expensive biomarker testing. Retinal biomarkers could play a pivotal role in large-scale screening, and serve as a first step in a multi-stage biomarker testing process, similar to other disease states such as cancer, cardiovascular disease, and diabetes. It is important to note that to truly validate retinal imaging as an AD screening tool, we will have to develop biomarkers that are specific to AD pathology. As health co-morbidities, specifically cardiovascular disease and diabetes, increase with age, it is not uncommon for older adults to present with multiple pathologies that affect the retina. However, aiming for a screening tool with high negative predictive value that can rule out low-risk older adults,

will be a valuable first screening stage. Retinal biomarkers have the potential to limit use of invasive and costly tests, such as brain imaging and cerebrospinal fluid sampling, and will help to precisely identify those at high risk for AD when a disease-modifying therapy becomes available.

CONFLICTS OF INTEREST

Dr. A. Kashani is a consultant to Carl Zeiss Meditec, and he has received both consulting fees and grant support from that company. Dr. D.C. DeBruc, with the University of Miami, has filed a provisional patent for a novel technology that is related to the topic of this article, although her specific invention is not reviewed herein. The authors have no other financial or material conflicts of interest to disclose.

REFERENCES

- Snyder PJ, Alber J, Alt C, et al. Retinal imaging in Alzheimer's and neurodegenerative diseases. *Alzheimer's Dement*. 2020.
- Alber J, Goldfarb D, Thompson LI, et al. Developing retinal biomarkers for the earliest stages of Alzheimer's disease: what we know, what we don't, and how to move forward. *Alzheimer's Dement*. 2020;16:229-243.
- Petersen RC, Aisen PS, Beckett LA, et al. Alzheimer's disease neuroimaging initiative (ADNI): clinical characterization. *Neurology*. 2010;74:201-209.
- Kennedy R, Schneider L, Cutter G. Biomarker positive and negative subjects in the ADNIS cohort: clinical characterization. *Curr Alzheimer Res*. 2012;9:1135-1141.
- Risacher S, Saykin A, Wes J, Shen L, Firpi H, McDonald B. Baseline MRI predictors of conversion from MCI to probable AD in the ADNI cohort. *Curr Alzheimer Res*. 2009;6:347-361.
- Ellis KA, Bush AI, Darby D, et al. The Australian Imaging, Biomarkers and Lifestyle (AIBL) study of aging: methodology and baseline characteristics of 1112 individuals recruited for a longitudinal study of Alzheimer's disease. *Int Psychogeriatrics*. 2009;21:672-687.
- Bressler SB, Edwards AR, Chalam KV, et al. Reproducibility of spectral-domain optical coherence tomography retinal thickness measurements and conversion to equivalent time-domain metrics in diabetic macular edema. *JAMA Ophthalmol*. 2014;132:1113-1122.
- Liu YL, Hsieh YT, Chen TF, et al. Retinal ganglion cell-inner plexiform layer thickness is nonlinearly associated with cognitive impairment in the community-dwelling elderly. *Alzheimer's Dement Diagnosis. Assess Dis Monit*. 2019;11:19-27.
- Yap T, Donna P, Almonte M, Cordeiro M. Real-time imaging of retinal ganglion cell. *Apoptosis Cells*. 2018;7:60.
- Braaf B, Donner S, Nam AS, Bouma BE, Vakoc BJ. Complex differential variance angiography with noise-bias correction for optical coherence tomography of the retina. *Biomed Opt Express*. 2018;9:486.
- Szigeti A, Tátrai E, Varga BE, et al. The effect of axial length on the thickness of intraretinal layers of the macula. *PLoS One*. 2015;10:1-11.
- Bennett AG, Rudnicka AR, Edgar DF. Improvements on Littmann's method of determining the size of retinal features by fundus photography. *Graefes. Arch Clin Exp Ophthalmol*. 1994;32:361-367.
- den Haan J, Verbraak FD, Visser PJ, Bouwman FH. Retinal thickness in Alzheimer disease? A systematic review and meta-analysis. *Alzheimer's Dement Diagnosis. Assess Dis Monit*;2017:1-9.
- Chan VTT, Sun Z, Tang S, et al. Spectral-Domain OCT Measurements in Alzheimer's disease. *Ophthalmology*. 2019;126:497-510.
- Wong BM, Cheng RW, Mandelcorn ED, et al. Validation of optical coherence tomography retinal segmentation in neurodegenerative disease. *Transl Vis Sci Technol*. 2019;8:6.
- Gao LY, Liu Y, Li XH, Bai QH, Liu P. Abnormal retinal nerve fiber layer thickness and macula lutea in patients with mild cognitive impairment and Alzheimer's disease. *Arch Gerontol Geriatr*. 2015;60:162-167.
- Cunha JP, Moura-Coelho N, Proença RP, et al. Alzheimer's disease: a review of its visual system neuropathology. Optical coherence tomography—a potential role as a study tool in vivo. *Graefes. Arch Clin Exp Ophthalmol*. 2016.
- Garcia-Martin ES, Rojas B, Ramirez AI, et al. Macular thickness as a potential biomarker of Mild Alzheimer's disease. *Ophthalmology*. 2014;121:1149-1151. e3.
- Bulut M, Yaman A, Erol MK, et al. Choroidal thickness in patients with mild cognitive impairment and Alzheimer's type dementia. *J Ophthalmol*. 2016;2016. <https://doi.org/10.1155/2016/7291257>.
- Cunha JP, Proença R, Dias-Santos A, et al. Choroidal thinning: alzheimer's disease and aging. *Alzheimer's Dement Diagnosis. Assess Dis Monit*. 2017;8:11-17.
- Dentchev T, Milam AH, Lee VM-Y, Trojanowski JQ, Dunaief JL. Amyloid-beta is found in drusen from some age-related macular degeneration retinas, but not in drusen from normal retinas. *Mol Vis*. 2003;9:184-190.
- Isas JM, Luibl V, Johnson LV, et al. Soluble and mature amyloid fibrils in drusen deposits. *Investig Ophthalmol Vis Sci*. 2010;51:1304-1310.
- Snyder PJ, Johnson LN, Lim YY, et al. Nonvascular retinal imaging markers of preclinical Alzheimer's disease. *Alzheimer's Dement Diagnosis. Assess Dis Monit*. 2016.
- Jiang J, Wang H, Li W, Cao X, Li C. Amyloid plaques in retina for diagnosis in Alzheimer's patients: a meta-analysis. *Front Aging Neurosci*. 2016;8:1-8.
- Koronyo-Hamaoui M, Koronyo Y, Ljubimov AV, et al. Identification of amyloid plaques in retinas from Alzheimer's patients and noninvasive in vivo optical imaging of retinal plaques in a mouse model. *Neuroimage*. 2011;54:S204-17.
- Koronyo Y, Biggs D, Barron E, et al. Retinal amyloid pathology and proof-of-concept imaging trial in Alzheimer's disease. *JCI Insight*. 2017;2:1-19.
- Haan J den, van deKreeke JA, Konijnenberg E, Kate Mten, et al. Retinal thickness as a potential biomarker in patients with amyloid-proven early- and late-onset Alzheimer's disease. *Alzheimer's Dement Diagnosis. Assess Dis Monit*. 2019;11:463-471.
- Cabrera DeBuc D, Somfai GM, Arthur E, Kostic M, Oropesa S, Mendoza Santiesteban C. Investigating multimodal diagnostic eye biomarkers of cognitive impairment by measuring vascular and neurogenic changes in the retina. *Front Physiol*. 2018;9:1-16.
- Arthur E, Somfai GM, Kostic M, Oropesa S, Santiesteban CM, DeBuc DC. Distinguishing cognitive impairment by using singularity spectrum and lacunarity analysis of the retinal vascular network. *Neurophotonics*. 2019;6:1.
- Jerman T, Pernus F, Likar B, Spiclin Z. Enhancement of Vascular structures in 3D and 2D angiographic images. *IEEE Trans Med Imaging*. 2016;35:2107-2118.
- Jerman T, Pernuš F, Likar B, Špiclin Ž. Blob enhancement and visualization for improved intracranial aneurysm detection. *IEEE Trans Vis Comput Graph*. 2016;22:1705-1717.
- Xu X, Xu S, Jin L, Song E. Characteristic analysis of Otsu threshold and its applications. *Pattern Recognit Lett*. 2011;32:956-961.
- Arthur E, Papay JA, Haggerty BP, Clark CA, Elsner AE. Subtle changes in diabetic retinas localised in 3D using OCT. *Ophthalmic Physiol Opt*. 2018;38:477-491.
- Țălu Ș. Multifractal geometry in analysis and processing of digital retinal photographs for early diagnosis of human diabetic macular edema. *Curr Eye Res* 2013;38:781-792.

35. Stošić T, Stošić BD. Multifractal analysis of human retinal vessels. *IEEE Trans Med Imaging*. 2006;25:1101-1107.
36. Kashani AH, Chen CL, Gahm JK, et al. Optical coherence tomography angiography: a comprehensive review of current methods and clinical applications. *Prog Retin Eye Res*. 2017;60:66-100.
37. Cabrera DeBuc D, Gaca-Wysocka M, Grzybowski A, Kanclerz P. Identification of retinal biomarkers in Alzheimer's disease using optical coherence tomography: recent insights, challenges, and opportunities. *J Clin Med*. 2019;8:996.
38. Ometto G, Moghul I, Montesano G, et al. Relayer: a free, online tool for extracting retinal thickness from cross-platform OCT images. *Transl Vis Sci Technol*. 2019;8(3):25.
39. Abramoff MD, Mullins RF, Lee K, et al. Human photoreceptor outer segments shorten during light adaptation. *Invest Ophthalmol Vis Sci*. 2013;54:3721-3728.
40. Messner A, Werkmeister RM, Seidel G, Stegmann H, Schmetterer L, Aranha dos Santos V. Light-induced changes of the subretinal space of the temporal retina observed via optical coherence tomography. *Sci Rep*. 2019;9:1-10.
41. O'Bryant SE, Mielke MM, Rissman RA, et al. Blood-based biomarkers in Alzheimer disease: current state of the science and a novel collaborative paradigm for advancing from discovery to clinic. *Alzheimer's Dement*. 2017;13:45-58.
42. Schott R. How do OCT devices for glaucoma compare. *Rev Optom*. 2020;157:32-43.
43. Yang Q, Reisman CA, Wang Z, et al. Automated layer segmentation of macular OCT images using dual-scale gradient information. *Opt Express*. 2010;18:21293.

How to cite this article: Alber J, Arthur E, Sinoff S, et al. A recommended "minimum data set" framework for SD-OCT retinal image acquisition and analysis from the Atlas of Retinal Imaging in Alzheimer's Study (ARIAS). *Alzheimer's Dement*. 2020;12:e12119. <https://doi.org/10.1002/dad2.12119>